Silicon Baroreceptors:

Modeling Cardiovascular Pressure Transduction in Analog VLSI

John Lazzaro *
Department of Computer Science
California Institute of Technology
Pasadena, California, 91125

James S. Schwaber
Wade T. Rogers
E. I. Du Pont de Nemours and Co.
Neural Computation Laboratory
Experimental Station
Wilmington, Delaware 19898

Abstract

This paper describes an analog VLSI model of the representation of blood pressure used in a neural control system in the cardiovascular system. The chip computes the representation in real time, using analog continuous-time processing. We apply a variety of pressure signals to the chip, confirming that the chip models known physiological responses. We are modeling this representation as a first step to understanding the neural computation of cardiovascular control; we hope to apply this knowledge to nonlinear dynamical control problems in the chemical industry.

1 Introduction

Many electrical engineers and computer scientists regard biological organisms as existence proofs for practical solutions to a variety of difficult computational problems. In the same way, many chemical engineers hope to learn practical techniques in chemical plant design and control from studying biological organisms. The cardiovascular and respiratory systems act together to extract oxygen from the air, distribute oxygen throughout the body through blood flow, carry unneeded carbon dioxide back to the lungs, and expel carbon dioxide out of the body.

* Present address: John Lazzaro, University of Colorado at Boulder, Campus Box 425, Boulder, Colorado, 80309–0425

The oxygen demands of the body are not static, but vary in response to physical exertion, digestion, and stress, for example. The body has a variety of control systems to dynamically regulate blood flow throughout the body in response to these internal and external factors. Several of these control systems are neural control systems; these systems involve sensing an aspect of cardiovascular state, transmitting this state information to the brain, computing the appropriate changes in cardiovascular state, and transmitting these changes to the appropriate muscular elements. This neural control is directly comparable to process control in a chemical plant, where sensors relay state information about the plant to a central computer that computes appropriate changes in state, and transmits the changes to elements such as valves and pumps.

The baroreceptor reflex is the cardiovascular neural control system we have chosen to study from this interdisciplinary perspective[8]. In this system, baroreceptors measure the blood pressure in a major blood vessel leading to the head, the carotid artery. Nerve fibers from the baroreceptors connect to neural circuits in the brainstem. These circuits act as a control system; the outputs from these circuits connect to the heart, and affect the rate of the heartbeat, and the volume of blood pumped with each heartbeat. The reflex also controls the allocation of the blood supply throughout the body; reflex outputs innervate the major body organs and regulate local resistance to blood flow. The neural circuits of the baroreceptor reflex receive additional inputs from other areas of the brain, including emotional and memory areas; however, reflex action persists if these additional inputs are cut.

Input representation is a crucial aspect of any neural system; understanding retinotopic organization is an essential prerequisite for deciphering primary visual cortex, and an appreciation of cochlear structure and function must precede an understanding of higher auditory structures. We began our research effort of the carotid sinus baroreceptor reflex by constructing a functional model of the baroreceptors in the carotid vessel. Inspired by recent work in silicon models of the cochlea [3] and the retina [4], we designed and tested a CMOS integrated circuit that models the baroreceptors; this paper reports on this chip. The circuit operates in real time using analog continuous-time processing.

2 Biological Baroreceptors

Mammals such as rats, dogs, and cats are common experimental animals for baroreceptor research; much of the data we used in our functional model comes from experiments using these animals. Baroreceptor function is qualitatively similar across these species; the quantitative details of baroreceptor response depends on the type of animal. There are 60-140 A-fiber baroreceptors in the carotid vessel of the rat. Each baroreceptor connects to a nerve fiber that sends signals to neural circuits in the brainstem. The fibers send signals using fixed-width, fixed-height pulses called action po-

tentials; information is carried in the rate and temporal position of action potentials[2].

Each baroreceptor k is tuned to a specific blood pressure V_k, in the range 40–180 mmHg. If the static blood pressure is less than the threshold pressure V_k, the baroreceptor fires at a low spontaneous rate or is silent. If the static blood pressure is greater than V_k, the firing rate of the baroreceptor increases approximately linearly with blood pressure, for pressures 10-30 mmHg greater than V_k. The baroreceptor firing rate saturates at a constant value for higher static blood pressures. In the dog, spontaneous rates are typically 0–20 spikes per second; saturated firing rates are typically 40-70 spikes per second [2].

It is valid to question the relevancy of static measurements of baroreceptors to a functional cardiovascular system; a static pressure implies a lack of heartbeats, certainly not a desired system state! The response of a baroreceptor to a step increase in pressure from below V_k to above V_k reveals a stereotypical dynamic behavior. Before the step, the baroreceptor fires at a low spontaneous rate. After the pressure step, the firing rate quickly increases to an instantaneous firing rate of 60–250 spikes per second, depending on step height. Over the next 200 ms, the firing spike rate exponentially decays to an asymptotic value, corresponding to the firing rate of the baroreceptor at the static pressure of the step height[2].

In a functional cardiovascular system, the baroreceptors typically encode neither static pressure or pressure steps, but a repetitive low frequency pressure waveform corresponding to a steady heartbeat. In addition, in a functional cardiovascular system, neural control circuitry does not receive input from a single baroreceptor tuned to a particular pressure, but from an array of 60-140 baroreceptors tuned to different pressures spanning the physiologically plausible range. To better understand this encoding, we designed and tested an array of silicon baroreceptors with the static and dynamic properties described in this section.

3 Silicon Baroreceptors

Figure 1 shows the architecture of the baroreceptor chip. An array of identical baroreceptor circuits receive a voltage V that represents pressure, apart from a proportionality constant. Each baroreceptor circuit k also receives an input that sets the threshold voltage V_k. A polysilicon resistor spans the length of the chip, and connects to the threshold input of each baroreceptor circuit. A voltage gradient across this resistor creates a linear threshold gradient across the baroreceptor array. The baroreceptor array outputs are the final outputs of the chip.

Figure 2 shows the baroreceptor circuit. The pressure input V and the threshold input V_k connect to a half-wave rectifier circuit, operating in the subthreshold region [5]. If $V < V_k$, no output current is produced; if $V > V_k$

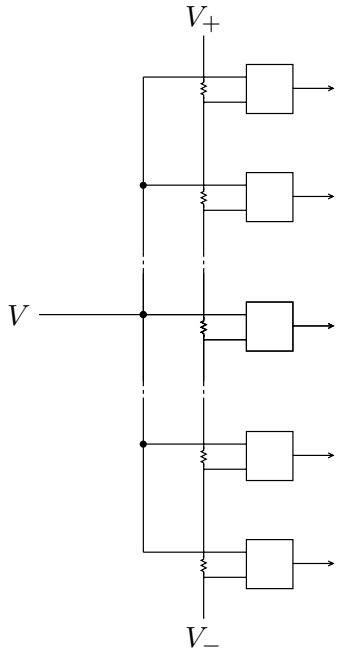

Figure 1. Figure shows block diagram of the chip. Input pressure, represented by the voltage V, is distributed to the array of silicon baroreceptors; each unmarked box represents a baroreceptor circuit. Each circuit also receives a programming voltage that sets the pressure threshold of the silicon baroreceptor. This programming voltage is tapped from a polysilicon resistor that spans the baroreceptor array. A voltage gradient on this resistor, applied with potentials V_+ and V_-, programs a different threshold for each circuit.

the output current of the circuit is

$$I_s \tanh(\frac{V - V_k}{V_o}).$$

The current I_s is an exponential function of the voltage V_a. In a standard transconductance amplifier, $V_o = 2kT/q\kappa$, where T is temperature, k and q are physical constants, and κ is a fabrication parameter. In a typical MOSIS 2μ process, V_o is 80 mV. We used a novel capacitive divider structure [M. Sivilotti, personal communication] on the transconductance amplifier in the rectifier circuit to increase the value of V_o, and thus widen the linear range of the rectifier.

The output of the rectifier circuit connects to a neuron circuit[6] that converts the input current into a pulse representation. The circuit has a fixed pulse width set by a control voltage. These pulses are the output of the baroreceptor circuit. These pulses are also connected to a feedback circuit that models the dynamic adaptation of biological baroreceptors.

The capacitor voltage V_A is the state variable for adaptation. This voltage is reduced by a diode structure, producing V_a, the control voltage of the rectifier. The current source I_l is gated by the baroreceptor output; during a pulse, I_l acts to decrease the state voltage V_A. The leak current I_h acts to reset the state voltage V_A to the quiescent value V_h; in normal operation, $I_h < I_l$. A PFET operating in the subthreshold region implements I_h; an NFET operating in the subthreshold region implements I_l.

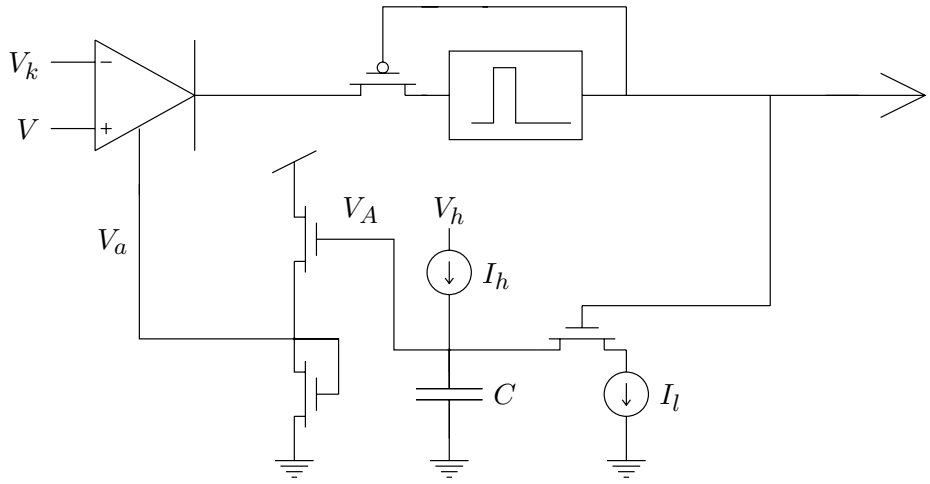

Figure 2. Figure shows the schematic diagram of the baroreceptor circuit. Pressure input and pressure threshold voltages V and V_k connect to a half-wave rectifier circuit [5]. The current output from the rectifier connects to a neuron circuit [6] that converts the current into fixed-width, fixed-height pulses. These pulses are the output of the circuit, and also are the input to a feedback loop that implements adaptation. The capacitor C holds the adaptation state voltage V_A; V_a, a scaled version of the voltage V_A, connects to the rectifier control input. Gated current source I_l and constant current source I_h change the potential V_A; the voltage V_h sets the quiescent value of V_A.

To qualitatively understand the circuit, consider the starting condition $V < V_k$. Because the rectifier circuit produces no output current under these conditions, the neuron circuit does not produce any pulses, and the current source I_l has no effect on V_A. Thus in the steady state, $V_a = 0.5V_A = 0.5V_h$, neglecting the back-gate effect on the diode structure.

Circuit behavior changes if V is rapidly increased to be greater than V_k. In this case, the rectifier circuit begins to produce current; for a large step that saturates the rectifier, it produces a current $I_s(V_a = 0.5V_h)$. This

current eventually causes the neuron circuit to produce a pulse. For the duration of the pulse, however, the state voltage V_A is reduced by the current source I_l. After the pulse finishes, the neuron circuit again accumulates charge from the rectifier circuit, but the rectifier produces a current $I_s(V_a < 0.5V_h)$, and thus the integration time necessary to produce a pulse increases. For an appropriate setting of I_l, I_h, and V_h, the neuron circuit continues to produce pulses at a progressively decreasing rate, until a steady-state firing rate is reached. In this way, the circuit models the adaptive behavior of a baroreceptor.

As derived in the Appendix, the steady-state firing rate of the baroreceptor circuit in this case is $I_h/(\tau_p I_l)$, where τ_p is the width of a neuron pulse. Also in the Appendix is a derivation of a recurrence relation that predicts the value of V_A at the start of the pulse $i+1$, given the value of V_A at the start of the pulse i. This recurrence relation is

$$V_{A,i+1} = V_{A,i} - (\tau_p/C)(i_l - i_h) + b\exp(-V_{A,i}/(2V_o)),$$

where C is the adaptation capacitance and b is

$$\frac{Q_f I_h}{C I_o}\exp(\frac{\tau_p(i_l - i_h)}{2V_o C}),$$

where Q_f is the charge needed by the neuron circuit to produce a pulse, and I_o is the fabrication constant in the expression $I_o\exp(V_{gs}/V_o)$ that defines subthreshold NFET transistor operation. This expression shows that V_A decreases linearly with each pulse until V_A becomes small enough for the $\exp(-V_{A,i}/(2V_o))$ term to have an effect.

Given the value of V_A at the start of a pulse, the equation

$$t_f = \frac{Q_f}{I_o}\exp(-V_{A,i}/(2V_0))\exp(\tau_p(I_l - I_h)/(2CV_0))$$

predicts the time between the end of that pulse and the beginning of the next pulse. This equation, also derived in the Appendix, coupled with the recurrence relation above, completely defines the step response of the baroreceptor. A solution to the recurrence relation would result in a closed form solution of the baroreceptor response.

4 Data

The chip was fabricated through MOSIS using a 2 μm n-well low-noise analog process. We fabricated an array of 28 baroreceptors. 7 outputs were directly brought off chip with pads; a multiplexer circuit enabled the sequential access of all 28 baroreceptors. The adaptation voltage V_A of several baroreceptor circuits was also brought off chip.

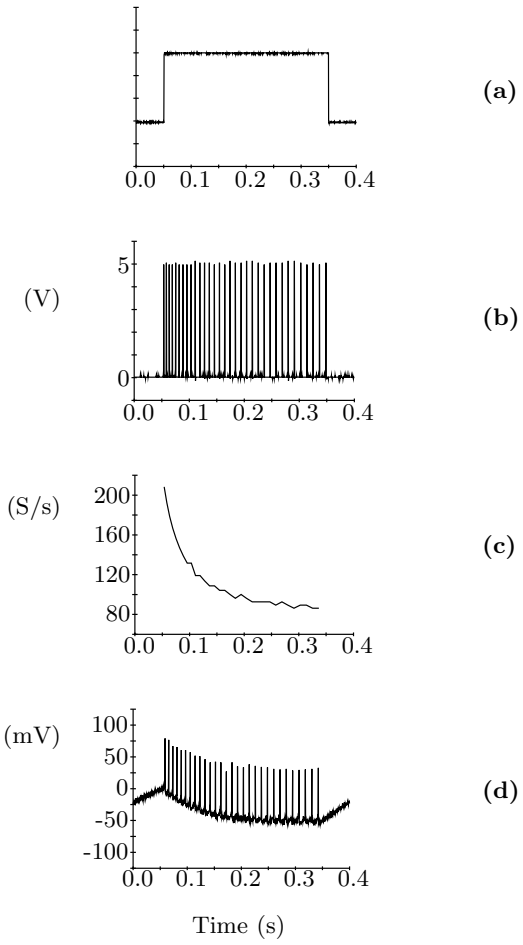

Figure 3. Plots show the step response of the baroreceptor circuit. **(a)** Plot shows the input voltage step. **(b)** Plot shows a baroreceptor circuit output. **(c)** Plot shows instantaneous firing rate of spikes in (b). **(d)** Plot shows the adaptation voltage V_A for the baroreceptor circuit. Voltage units are relative to average value of waveform.

We set the control voltages and currents on the chip so that the step response of the silicon baroreceptors was similar to biological data; in specific, we matched the saturated firing rate, initial instantaneous firing rate, and adaptation time constant of the circuit to the biological responses. We set the threshold voltages V_k for the baroreceptor array to span 3V, from 1V to 4V. Figure 3 shows the step response of the baroreceptor circuit. Figure 3(a) shows the input step; the low voltage of the step is below the threshold of the measured baroreceptor, and the high voltage of the step is above the saturation voltage of the rectifier circuit of the measured baroreceptor.

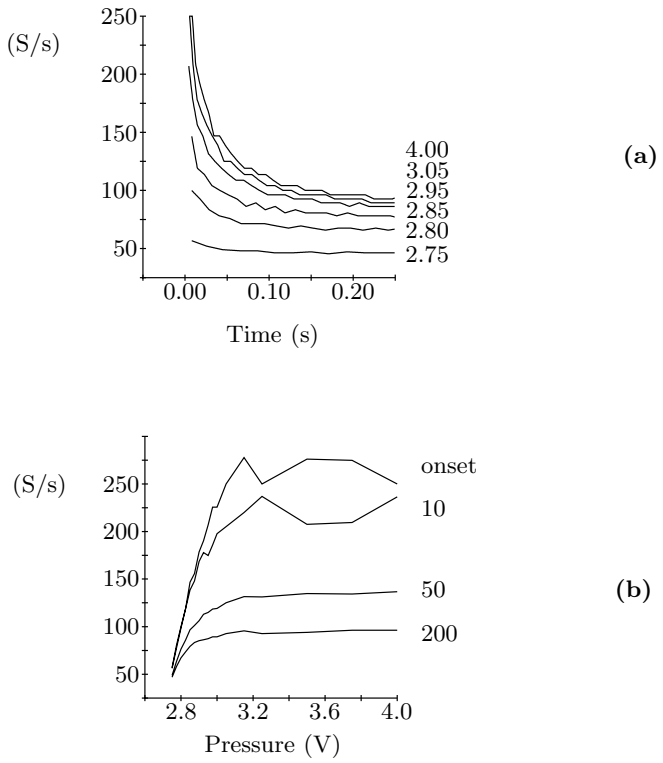

Figure 4. Plots show the step response of the baroreceptor circuit, for various step sizes. **(a)** Plot shows the instantaneous spike rate of step response as a function of time for various step heights. Labels on right indicate step height in volts; all steps begin at ground. **(b)** Plot shows instantaneous spike rate at particular times during the step response of (a), as a function of step height. Labels on right indicate the time of each plot, in seconds.

Figure 3(b) shows the raw baroreceptor output. As desired, the initial pulses are spaced closely together, but later pulses are spaced father apart. Figure 3(c) shows the instantaneous firing rate of the data in Figure 3(b). The circuit starts firing at approximately 200 spikes per second, and decays to about 80 spikes per second; the firing rate is halved in about 100 ms. These values are similar to parameters measured from physiological baroreceptors [1,2,9].

Figure 3(d) shows the adaptation state voltage V_A for the baroreceptor circuit. The spikes on the waveform are a result of switching noise in the pulse feedback to V_A; this nonideality is not accounted for by the analysis in the previous section. Nontheless, the qualitative shape of curve is in agreement with the recurrence relation for V_A in the previous section; an initial linear decrease followed by an exponential decay.

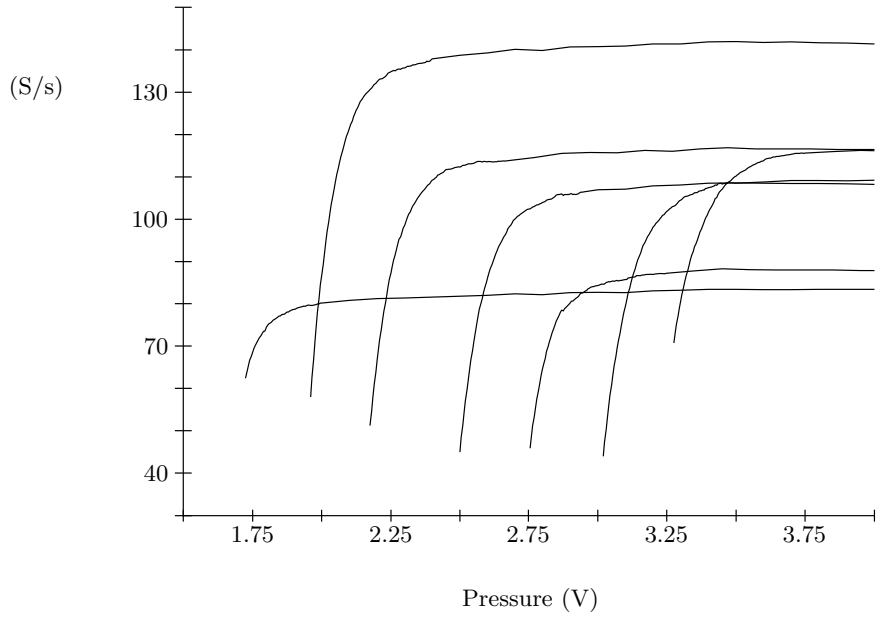

Figure 5. Plot shows the static response of seven baroreceptor circuits on the chip. Mean firing rate (spikes/second) is plotted against static pressure, in volts. Data was taken by applying a slow reverse ramp voltage waveform, and continuously measuring output.

Figure 4(a) shows the instantaneous spike rate of the step response of the baroreceptor circuit, for various step heights. Each step starts from ground; the label on the right of the figure shows the step height. The onset response of the circuit has the greatest gain; Figure 4(b) emphasizes this feature, by plotting the instantaneous spike rates for a particular time during the step response, for different size heights.

Figure 5 shows the static response of 7 baroreceptor circuits on the chip. To take this data, we used a very slow downward ramp voltage as input, and continuously measured the spike rate. The data shows a large variation in saturated firing rates, because of component mismatches between the different baroreceptor circuits. Nonetheless, the 7 baroreceptor circuits all exhibited the characteristic step response with identical control voltages applied to all circuits.

Figure 6 shows the output of the 7 baroreceptors circuits, in response to a low-frequency sinusoid. In this experiment, the valley of the sinusoid was fixed at 1V, and the peak of the sinusoid was systematically increased. Figure 6(a) shows a 2V peak. Only two baroreceptors are firing. Figure 6(b)

shows a 2.5V peak; several baroreceptors are firing. The spatiotemporal pattern of the outputs encodes the rising and falling edges of the waveform. Figures 6(c) and 6(d) show a 3V peak and a 3.5V peak respectively; more baroreceptors are firing, and the encoding of the rising and falling edges of the waveform is enhanced.

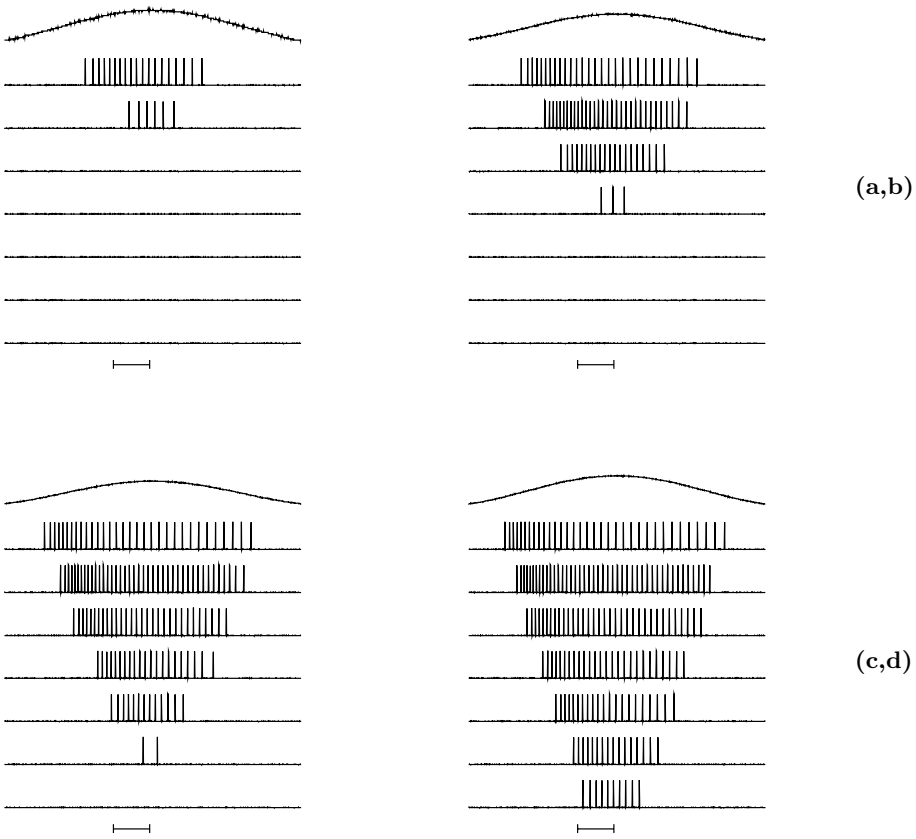

Figure 6. Plots show the output of 7 baroreceptor circuits, in response to a low frequency sinusoid. The time marker for each plot measures 50ms. For each plot, top spike trace is baroreceptor tuned to the lowest pressure (1), bottom spike trace is baroreceptor tuned for the highest pressure (7). Lowest point of sinusoid is at 1V for all plots. **(a)** Highest point of sinusoid is at 2V. **(b)** Highest point of sinusoid is at 2.5V. **(c)** Highest point of sinusoid is at 3V. **(d)** Highest point of sinusoid is at 3.5V.

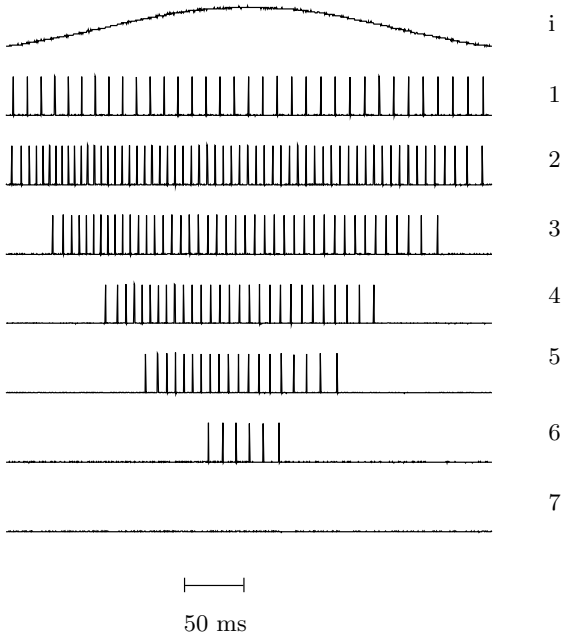

Figure 7. Plot shows the response of seven baroreceptor circuits to a low-frequency sinusoid; the lowest point of sinusoid is at 1.9V, the highest point of sinusoid is at 3.1 volts. All other aspects of figure are identical to Figure 6.

The starting and stopping of the baroreceptor firing is the primary encoding of the input waveform in Figure 6. A secondary encoding of the input waveform is found in the changing rate of firing of each circuit output. For baroreceptor circuits tuned to a pressure corresponding to a large rate of change in the input signal, for example trace 3 in Figure 6(d), spike rate adaptation occurs after the onset of the signal, similar to the step response of Figure 3(b). For circuits tuned to a pressure corresponding to a small rate of change of the input signal, for example trace 7 of Figure 6(d), this adaptation behavior is not seen. The time course of the pressure signal and the time constant of adaptation interact to produce a variety of responses between these two extremes, as seen in other traces in Figure 6.

Figure 7 shows the output of the 7 baroreceptor circuits in response to a slow sinusoid with valley of 1.9V and a peak of 3.1V. In response to this signal, some outputs are completely saturated, some fire continuously with a rate modulated by the input, some fire on part of a cycle, and some are always off. This variety of responses is physiologically normal; a functional cardiovascular system produces pressure waveforms that span only a fraction of the tuning of the baroreceptor array.

5 Discussion

To a first order, the chip is fully functional and computes the baroreceptor representation in real time. The major functional problem with the chip involves the slow adaptation time constant of the baroreceptor circuit. If excited with very slow pressure waveforms around the threshold voltage, the neuron circuit in the silicon baroreceptor does not function properly. The very small dV/dt produced on the integration capacitor of the neuron circuit is not sufficient to force an output pulse to occur, and the amplifier in the neuron circuit becomes temporarily biased in its linear range. As a result, current source I_l in the feedback circuit is no longer pulsed, but is always on, and the state variable V_A is no longer computed properly.

A neuron circuit optimized for low-frequency operation would solve this problem; this optimization involves improving the AC gain of the circuit. Another solution to the problem involves adding a second neuron circuit in series with the first neuron circuit, in a manner similar to the axon circuit of Mead [6]. In this axon circuit, the output of the first neuron stage must be fully on before the second neuron stage is activated. In this case, the linearly biased first neuron does not affect the feedback stage, and the slow rise time of the first neuron output is sharpened by the second neuron output.

The circuit is a simple model of baroreceptors; we omitted many aspects of baroreceptor function. In addition to the adaptation modeled by the chip, biological baroreceptors adapt their response over many minutes[7]. The transduction mechanism of baroreceptors may also sense the time derivative of pressure, in addition to instantaneous pressure, and present the weighted sum of dP/dt and P to the cell [1]; the silicon baroreceptors only sense instantaneous pressure. The chip models a generic baroreceptor; in actuality, there are several classes of baroreceptors[9]. These different classes vary in the extent of the linear range of response to static pressure. An improved baroreceptor circuit would model these additional aspects of behavior.

The responses shown in Figures 6 and 7 show the complexity of the baroreceptor encoding, and encourage the design of circuits that extract information from the representation. Several general methods of processing are possible. One method compares the temporal sequence of firing across the baroreceptor array, to encode the rising and falling edges of the pressure pulse. A second method examines the spike patterns of a single baroreceptor during a pressure pulse, examining the interaction between baroreceptor adaptation and the slope of the pressure waveform at threshold. A third method looks at the mean rate of firing of the baroreceptor array over many pressure pulses, to encode average pressure.

Examination of this representation suggests strategies for neural computation; by studying the neural circuitry that receives inputs from the baroreceptors, we can judge the plausibility of these strategies. The baroreceptor fibers connect to the second-order cells of the Nucleus Tractus Solitarius (NTS) in the brainstem. We are actively pursuing physiological and

anatomical studies on these neurons and other neural areas involved in the baroreceptor reflex.

6 Conclusions

We have designed and tested a silicon model of the baroreceptors of the carotid vessel. The chip computes the baroreceptor representation in real time, using analog continuous-time processing. The output of the chip suggests strategies for neural computation in the carotid sinus baroreceptor reflex.

7 Acknowledgements

We are grateful for C. Mead for providing financial support and laboratory facilities for chip design and testing, and K. Johnson for providing laboratory facilities for document preparation. We also thank the members of the Neural Computation Laboratory at Dupont, the Physics of Computation Laboratory at Caltech, and the OCP Laboratory at the University of Colorado at Boulder. This work was funded by Dupont, the Office of Naval Research, the Defense Advanced Research Projects Agency, and the State of California. MOSIS provided chip fabrication.

8 Appendix

This appendix provides derivations for several mathematical statements in the main text. Consider two consecutive pulses from a baroreceptor circuit. Define the first pulse to have a width τ_p, and define the time from the end of the first pulse to the start of the second pulse to be τ_f. Also, let the voltage V_A at the start of the first pulse be $V_{A,i}$ and the voltage V_A at the start of the second pulse be $V_{A,i+1}$. With these definitions we can write $V_{A,i+1}$ as a function of $V_{A,i}$, as

$$V_{A,i+1} = V_{A,i} + (I_h/C)(\tau_p + \tau_f) - (I_l/C)\tau_p, \tag{1}$$

where I_l, I_h, and C are the value of the components marked in Figure 2. If a steady state condition exists, $V_{A,i+1} = V_{A,i}$; the firing frequency is defined as $1/(\tau_p + \tau_f)$, and thus Equation 1 can be solved directly for the firing frequency, yielding the expression $I_h/(I_l\tau_p)$ as stated in the main text.

We next derive the recurrence relation that predicts the value of $V_{A,i+1}$ given $V_{A,i}$. During the time the first pulse is high, the neuron circuit is blocked from receiving charge from the rectifier circuit. After the first pulse has ended, the neuron circuit is reset, and needs Q_f charge to fire again. Also, after the first pulse has ended, $V_A = V_{A,i} + \tau_p(I_h - I_l)/C \equiv V_{A,f}$; this expression comes from letting $\tau_f = 0$ in Equation 1. The operation of the

neuron circuit from the time the first pulse ends to the time the second pulse begins can be expressed by the integral

$$Q_f = \int_0^{\tau_f} I_o \exp(V_{A,f}/(2V_o) + (I_h t)/(2CV_o))dt. \quad (2)$$

This equation describes the integration of charge Q_f by the neuron circuit; this charge comes from the saturated rectifier circuit, whose control voltage V_a is increasing during the charging period due to the current source I_h. The factor of 2 in the exponential models the diode structure that transforms V_A into V_a. Equation 2 can be solved for t_f, yielding

$$t_f = \frac{2CV_o}{I_h} \ln(\frac{Q_f I_h}{2I_o CV_o} \exp(-V_{A,f}/(2V_o)) + 1) \approx \frac{Q_f}{I_o} \exp(-V_{A,f}/(2V_o)). \quad (3)$$

This approximation is valid if $1 \gg ((Q_f I_h)/(2I_o CV_o)) \exp(-V_{A,f}/(2V_0))$. Substituting the definition of $V_{A,f}$ yields the final expression for t_f shown in the main text,

$$t_f = \frac{Q_f}{I_o} \exp(-V_{A,i}/(2V_0)) \exp(\tau_p(I_l - I_h)/(2CV_0)). \quad (4)$$

This expression can be combined with Equation 1 to yield, after rearrangement, the recurrence relation

$$V_{A,i+1} = V_{A,i} - (\tau_p/C)(i_l - i_h) + b \exp(-V_{A,i}/2V_o), \quad (5)$$

where b is

$$\frac{Q_f I_h}{C I_o} \exp(\frac{\tau_p(i_l - i_h)}{2CV_o}), \quad (6)$$

shown in the main text.

References

[1] M. W. Chapleau and F. M. Abboud, "Contrasting effects of static and pulsatile pressure on carotid baroreceptor activity in dogs," *Circulation Research,* vol. 61, no. 5, pp. 648-658, 1987.

[2] S. Landgren, "On the excitation mechanism of the carotid baroreceptors," *Acta Physiology Scandanavia,* vol. 26, pp. 1-34, 1952.

[3] R. F. Lyon and C. Mead, "An analog electronic cochlea," *IEEE Trans. Acoust., Speech, Signal Processing,* vol. 36, pp. 1119–1134, July 1988.

[4] C. Mead, *Analog VLSI and Neural Systems.* Reading, MA: Addison-Wesley, 1989, pp. 257-278.

[5] C. Mead, *Analog VLSI and Neural Systems.* Reading, MA: Addison-Wesley, 1989, pp. 88-90.

[6] C. Mead, *Analog VLSI and Neural Systems.* Reading, MA: Addison-Wesley, 1989, pp. 193-204.

[7] P. A. Munch, M. C. Andresen, and A. M. Brown "Rapid resetting of aortic baroreceptors in vitro," *American Journal of Physiology,* vol. 244, pp. H672-H680, 1983.

[8] J. S. Schwaber, "Neuroanatomical substrates of cardiovascular and emotional-autonomic regulation," in *Central and Peripheral Mechanisms of Cardiovascular Regulation ,* A. Magro, W. Osswald, D. Reis and P. Vanhoutte, Eds. New York: Plenum Publishing Company, 1986, pp. 353-384.

[9] J. L. Seagard, J. F. M. van Brederode, C. Dean, F. A. Hopp, L. A. Gallenberg, and J. P. Kampine, "Firing characteristics of single-fiber carotid sinus baroreceptors," in review.